ELSEVIER

Tectonophysics 354 (2002) 239–256

TECTONOPHYSICS

www.elsevier.com/locate/tecto

Stress modeling of tectonic blocks at Cape Kamchatka, Russia using principal stress proxies from high-resolution SAR: new evidence for the Komandorskiy Block

Sarah B.Z. McElfresh [a,*], William Harbert [a], Cheng-Yu Ku [b], Jean-Shang Lin [b]

[a] *Department of Geology and Planetary Science, University of Pittsburgh, 200 Space Res. Coordination Center, Pittsburgh, PA 15260, USA*
[b] *Department of Civil and Environmental Engineering, University Of Pittsburgh, Pittsburgh, PA, 15260 USA*

Received 25 July 2001; accepted 20 June 2002

Abstract

A new data set of 851 lineaments mapped from European Remote Sensing satellites 1 and 2 full resolution Synthetic Aperture Radar (SAR) data are interpreted as geological proxies for stresses resulting from plate and block collision near the Cape Kamchatka region of the Kamchatka Peninsula using a Geographical Information Systems-based analysis. Numerical Manifold Method (NMM) analysis is used to model the stress field within the Cape Kamchatka region resulting from the collision of lithospheric plates and blocks. Results of our NMM model, using different plate motion and plate configuration in the region, are compared with orientation data for the mapped set of lineaments. These data suggest that the lineaments observed in SAR cannot be fully explained by a simple two-plate model in this in the Cape Kamchatka region. As an alternative, we propose that the data can be explained by the existence of the previously proposed Komandorskiy Block. Recent Global Positioning Satellite measurements in the Aleutian Islands support our lineament-derived model and show that the near Islands/Komandorskiy Island block of the extreme western Aleutians is moving independently of the North American Plate.

Keywords: Kamchatka; Tectonics; SAR; Numerical modeling

1. Introduction

The Kamchatka Peninsula of northeastern Russia consists of zones of complexly deformed accreted terranes. The study area includes Cape Kamchatka and part of the Central Kamchatka Depression in the latitude–longitude range of 55.5–58.0°N to 159.9–163.3°E and is located on the eastern side of the Kamchatka Peninsula (Fig. 1). Presently, the Cape Kamchatka region is an area of intense tectonic activity with an unknown number of lithospheric plates and/or tectonic blocks interacting. Models consisting of two plates (e.g. Chapman and Solomon, 1976; Cook et al., 1986; Riegel et al., 1993), three plates (Cook et al., 1986; Riegel et al., 1993; Geist and Scholl, 1994), or two plates with numerous blocks (Mackey et al., 1997; Avé Lallemant and Oldow, 2000) have been proposed for this region. In this study, we determine the plate configuration in the

* Corresponding author. Tel.: +1-412-624-8779; fax: +1-412-624-3914.
E-mail address: sbzl@pitt.edu (S.B.Z. McElfresh).

0040-1951/02/$ - see front matter
PII: S0040-1951(02)00341-4

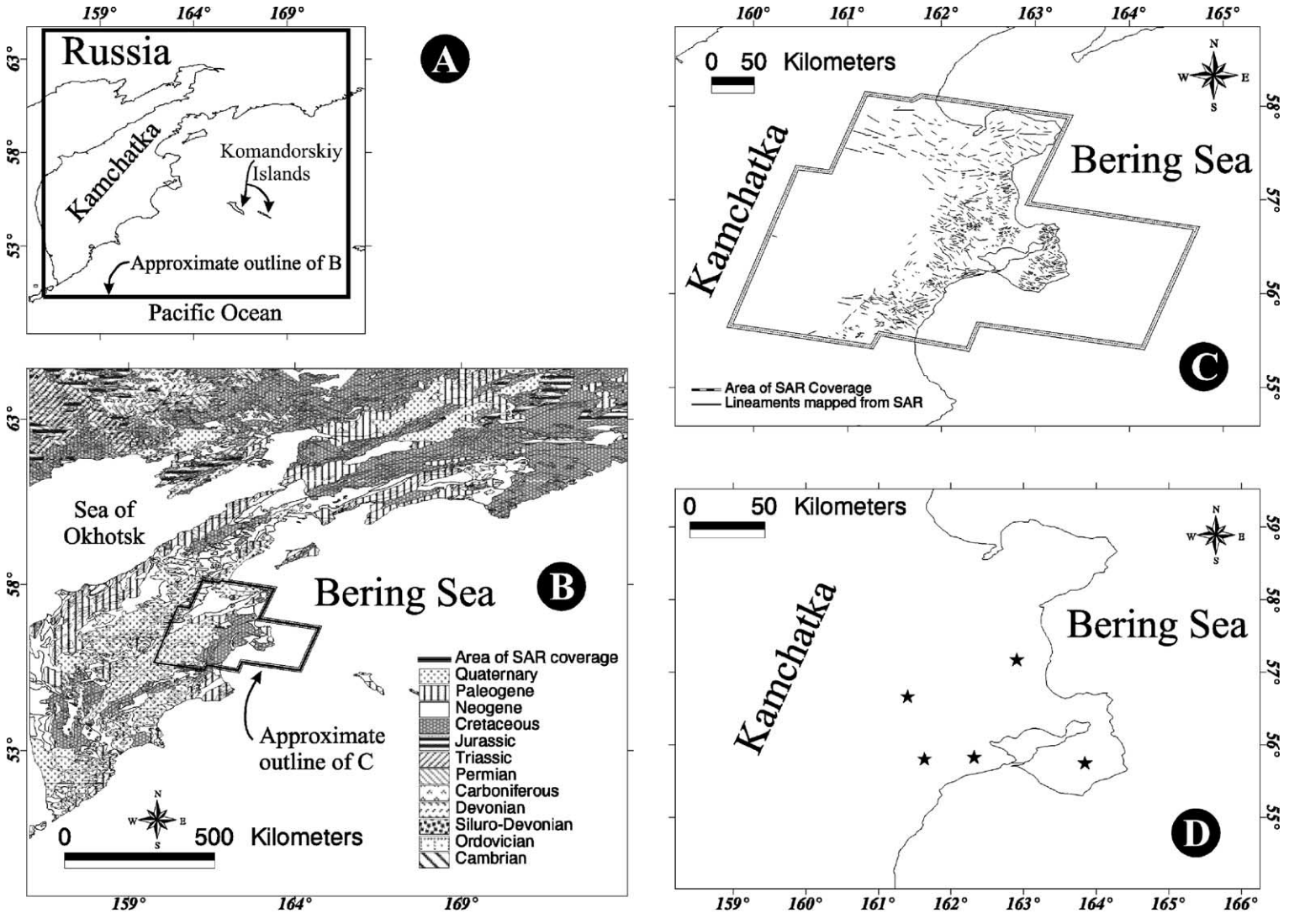

Fig. 1. (A) Regional map of the Kamchatka Peninsula. (B) Geology map of the study area, located within the SAR boundary (bounding rectangle of SAR 55.5–58.0°N, 159.9–163.3°E), using the geology coverages from AGI (1998). (C) Map showing SAR-mapped lineaments in the Cape Kamchatka region. (D) Locations of points at which linear plate velocities were calculated.

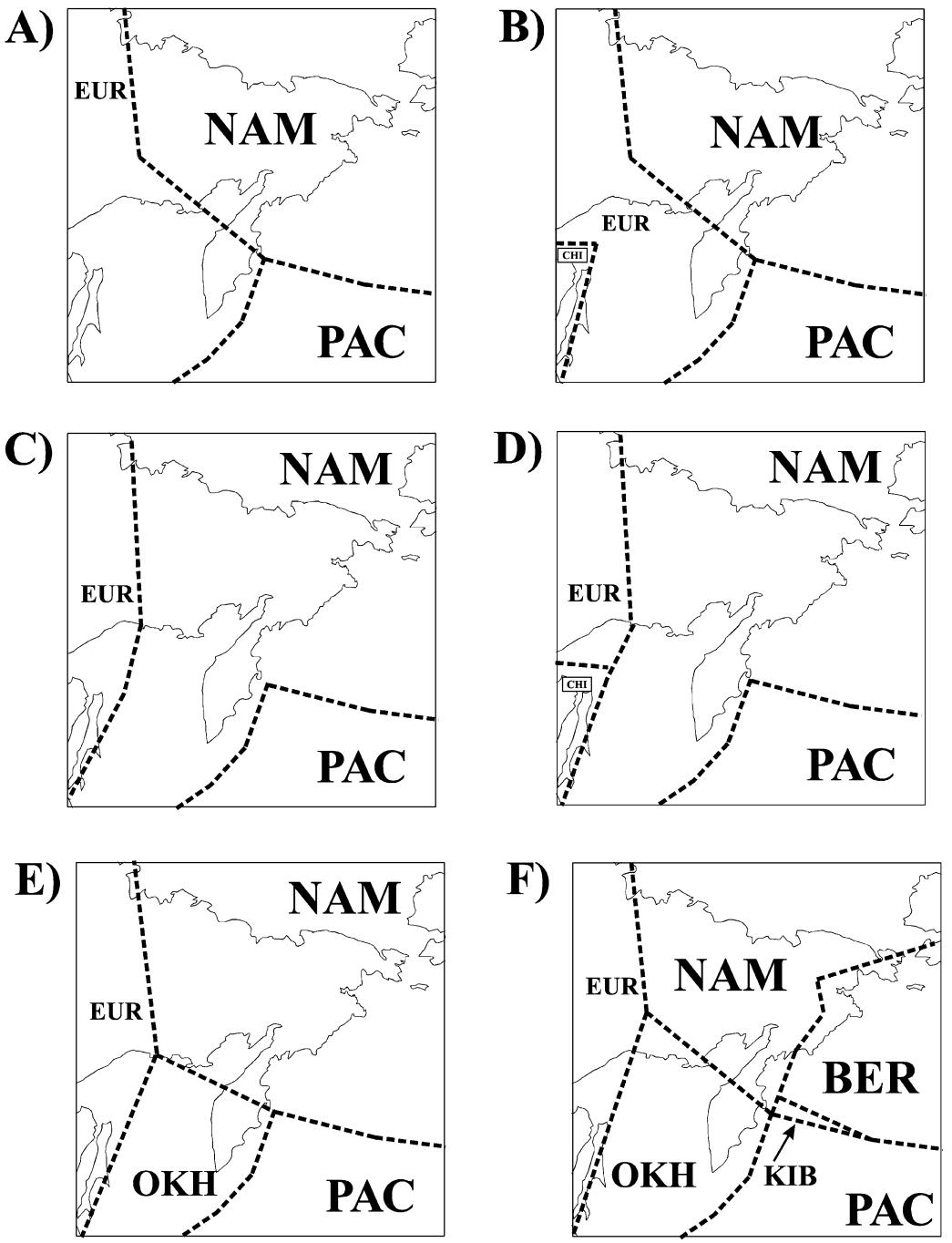

Fig. 2. Possible plate geometries within the Northwester Pacific Basin (Plates are, EUR: Eurasian; NAM: North American; PAC: Pacific; CHI: China; OKH: Okhotsk; BER: Bering, KIB: Komandorskiy Island Block). Configurations (A) through (E) are redrafted from Chapman and Solomon (1976). Configuration F is redrafted from Mackey et al. (1997).

northwestern Pacific basin in the region of Cape Kamchatka, Kamchatka Peninsula, Russia using lineaments mapped from full-resolution ERS-1 and ERS-2 synthetic aperture radar (SAR) data as an indicator for the orientation of the major stress axis (Zimmerman, 2000).

Previous models can be broadly classified into two-plate models in which only two plates are interacting in the Cape Kamchatka region and three-plate models in which three plates (or blocks) are interacting in this region. Numerous authors have discussed the number, location, and configuration of tectonic plates in the Pacific basin in terms of seismic data, paleomagnetic data, magnetic isochrons, and fault orientation data (Chapman and Solomon, 1976; Engebretson et al., 1984, 1985; Watson and Fujita, 1985; Grigoriev and Krylov, 1992; Heiphetz et al., 1992a,b; Didenko et al., 1993; Riegel et al., 1993; Geist and Scholl, 1994; Mackey et al., 1997; Perchesky et al., 1997; Levashova et al., 1998).

Chapman and Solomon (1976) examined five possible plate configurations for Kamchatka using seismicity and focal mechanisms (Fig. 2A–E). The configurations range from three to four plates being present in the northwestern Pacific with the position of a plate junction at, or offshore, from Cape Kamchatka. Their accepted model shows only a two-plate interaction at Cape Kamchatka (Fig. 2C). Riegel et al. (1993) use focal mechanisms and lineament data to invoke a three-plate configuration at Cape Kamchatka. On the basis of seismicity data, Mackey et al. (1997) introduce evidence for several tectonic blocks interacting at Cape Kamchatka (Fig. 2F). Examination of the components of each hypothesis in conjunction with geologic and geophysical evidence brings the picture only slightly more in focus. Complicating the matter further is that plate boundaries do not remain constant over time; thus, plates or blocks, which may have been present in the past, may no longer exist.

Of the models examined, most authors suggest that at any given time, only two plates were actively converging to form Kamchatka. Engebretson et al. (1984, 1985) favors a two-plate model based on the compilation of magnetic isochrons and fault orientation data used to determine velocity and orientation of the plates. Watson and Fujita (1985) confirm that the structural evidence of thrust and strike–slip faults matches the convergence of the Pacific and Eurasian plates. Riegel et al. (1993), however, notes that the orientation of lateral faults in Eurasia is inconsistent with this model. Our study provides additional data with reference to fault orientations at Cape Kamchatka through time to give additional insight on this question. Other hypotheses for the plate configuration of the northwestern Pacific include smaller tectonic blocks (Mackey et al., 1997; Avé Lallemant and Oldow, 2000; Gaeidicke et al., 2000). Mackey et al. (1997) proposes and provides evidence for a Bering Block and in their reconstruction shows other tectonic blocks. Global Positioning System results (Avé Lallemant et al., 1999; Oldow et al., 1999) suggest that the Near Island Block of the Aleutian Islands is moving independently at a rate of approximately 40% the rate of the Pacific plate (Avé Lallemant and Oldow, 2000). The goal of this study was to determine primary lineament structural data of this region in order to evaluate regional stress regimes. We then compared our data with numerical-model derived stress orientation data for a select set of possible plate configurations in the Cape Kamchatka region. After comparing observations with the predictions of various plate models, we strongly favor a three-block model in which the Okhotsk plate, Pacific plate and Komandorskiy block interact at Cape Kamchatka.

2. Methodology

In order to address questions about stresses and plate interactions in the tectonically active Cape Kamchatka region of the Kamchatka Peninsula, Russia, mapping of lineaments from ERS-1 and ERS-2 synthetic aperture radar images was undertaken. The SAR images were supplied by NASA and the Alaska SAR Facility. Each individual scene covers an area of 100×100 km. Full resolution images have 12.5 m pixel spacing with 30-m resolution. The images are projected on to an ellipsoid without considering differences in surface elevation to the true geoid. The ellipsoid surface used is the Goddard Earth Model-6 (GEM06) that assumes an equatorial radius of 6378.144 km and polar radius of 6356.755 km (Olmsted, 1994). The results of the mapping were combined with bedrock geology information and spatially analyzed using ESRI Arc/Info 7.0.4 and GRID, INFO, ArcEdit and ArcPlot modules. Earth

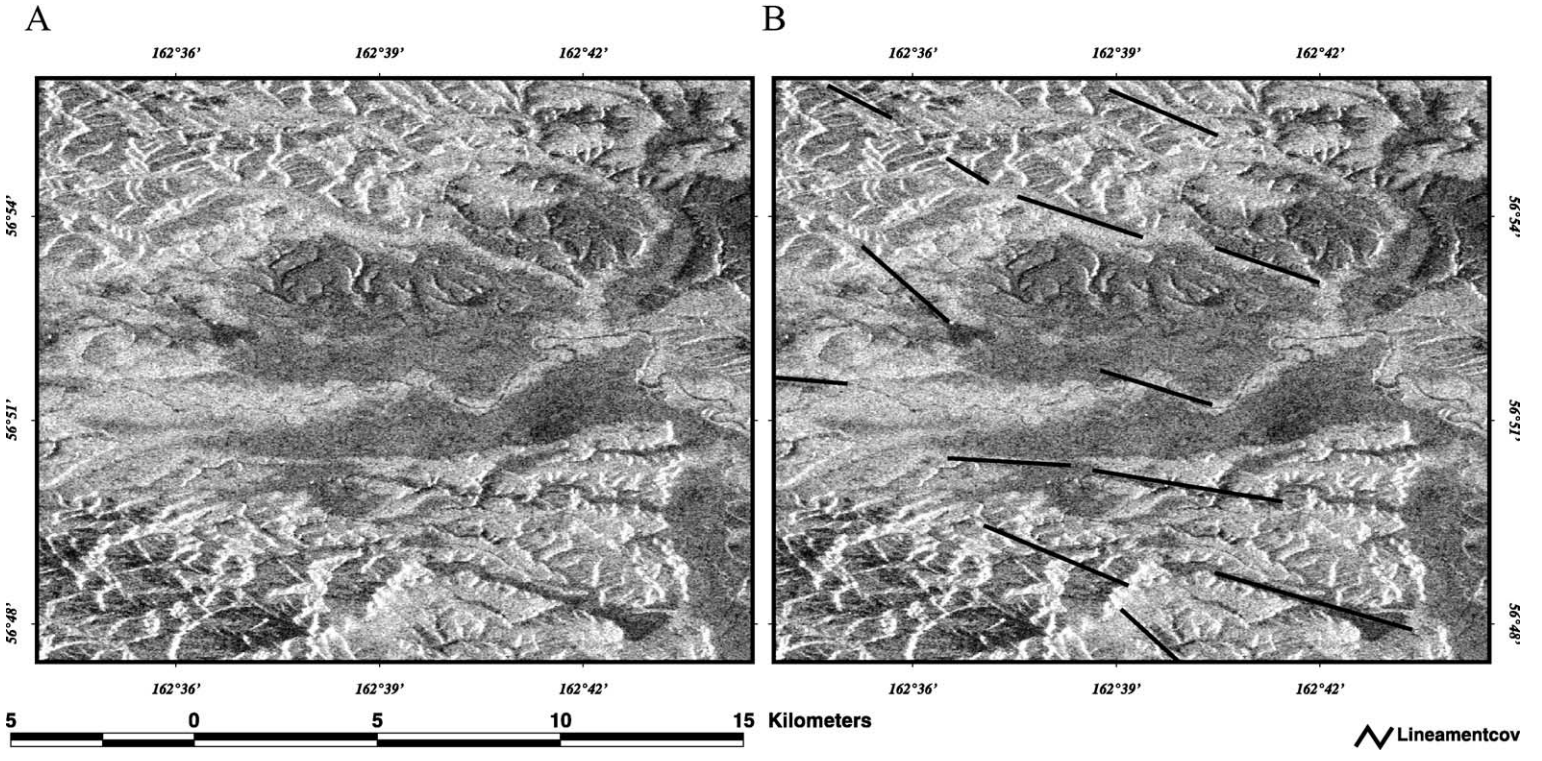

Fig. 3. (A) $0.2 \times 0.2^{\circ}$ SAR viewing window. (B) Same view lineaments (represented by Lineamentcov in B) mapped as interpreted from the SAR imagery.

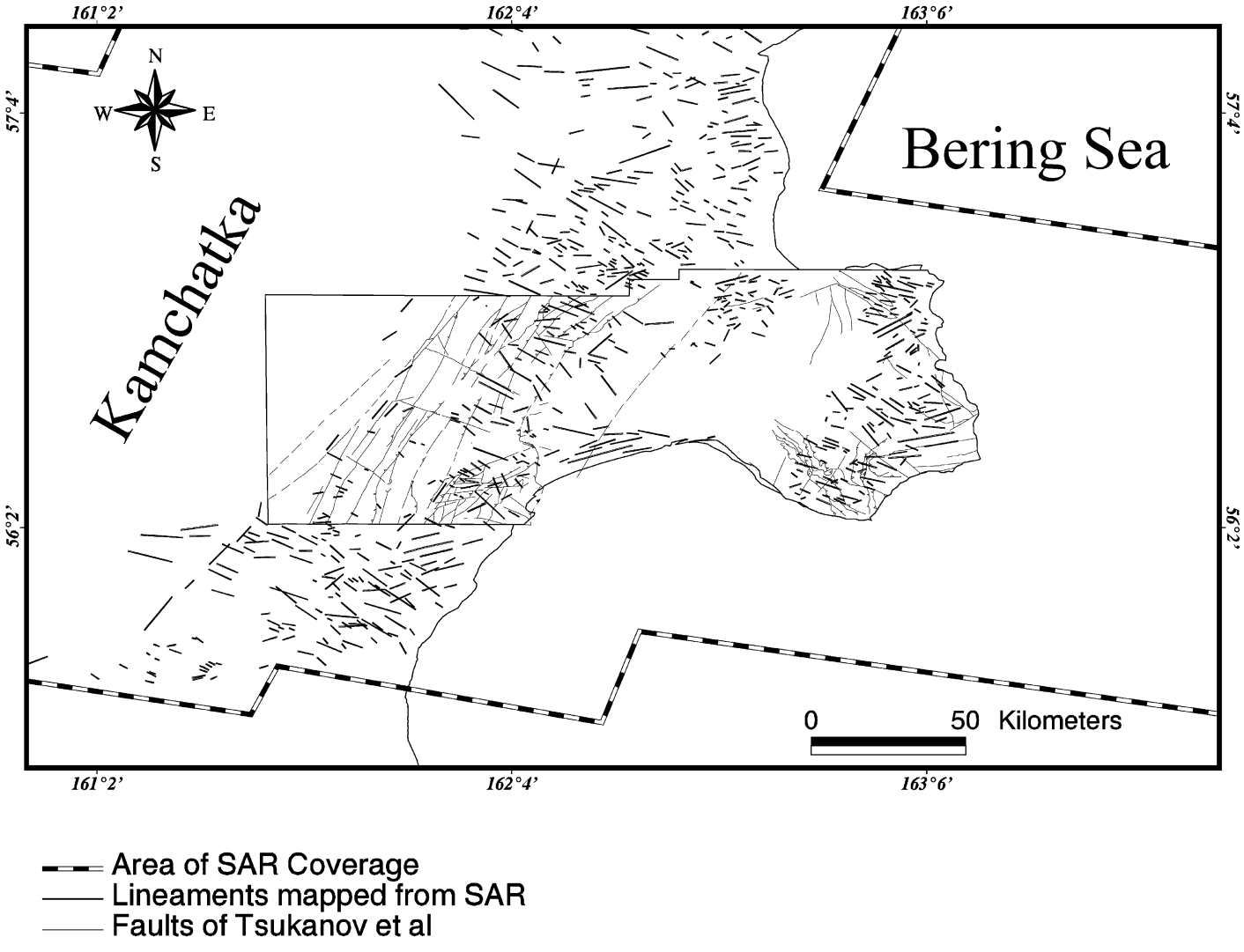

Fig. 4. Map depicting lineaments mapped from SAR compared with field based mapping of Tsukanov et al. This figure demonstrates the strong correlation between the lineaments mapped from radar and those mapped from field studies.

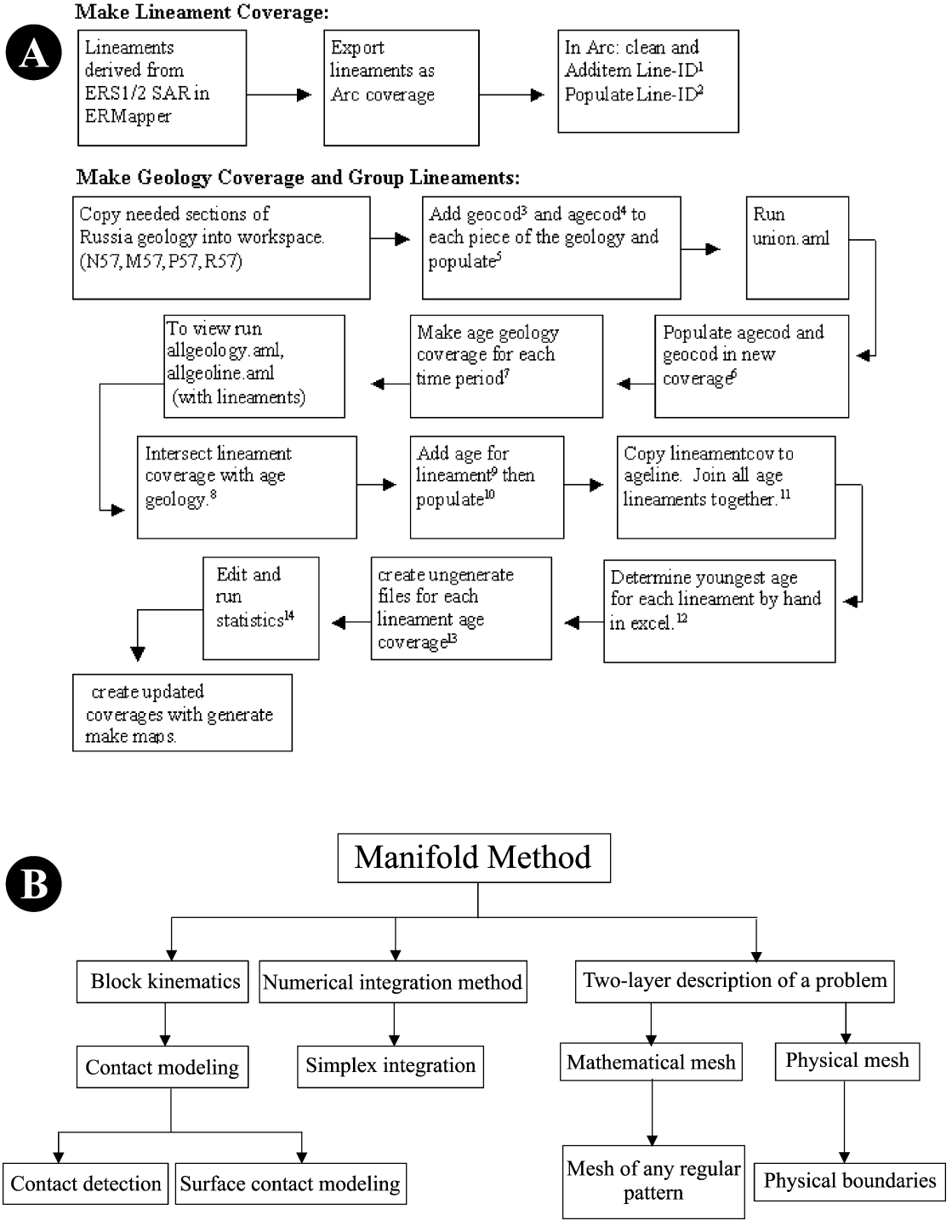

Fig. 5. (A) GIS processing steps for this analysis. Superscripts refer to specific Arc/Info commands described in Zimmerman (2000). (B) Flow chart depicting the structure of the NMM method as described in Ku (2001).

Resource Mapping ERMapper 5.5A software was also used to mosaic, optimize, and analyze the SAR images. For complete processing details, refer to Zimmerman (2000); an abbreviated methodology is presented below.

In this paper, a lineament is defined as a linear feature observable by a variation in radar backscatter in the high resolution SAR image when viewed in a $0.2 \times 0.2^{\circ}$ (UTM Zone 57 extents were approximately 22×22 km) viewing region (Fig. 3). Thrust faults are well documented in the Cape Kamchatka region and it is difficult to correctly represent the three-dimensional orientation and geometry of a thrust fault. This definition excludes the majority of thrust faults in the region due to their curvilinear nature, thereby reducing the overall number of thrust faults mapped in the region. We verified the mapping technique through a comparison of the lineament maps determined from radar data with field maps of Perchesky et al. (1997), Gaeidicke et al. (1998) and Tsukanov et al. (2002, personal communication) (Fig. 4). The location of faults from the field study maps and lineaments mapped from radar correspond well in the Eastern Kumroch range, and in the northern and southern regions of Cape Kamchatka. The faults and lineaments compare in spatial location and orientation.

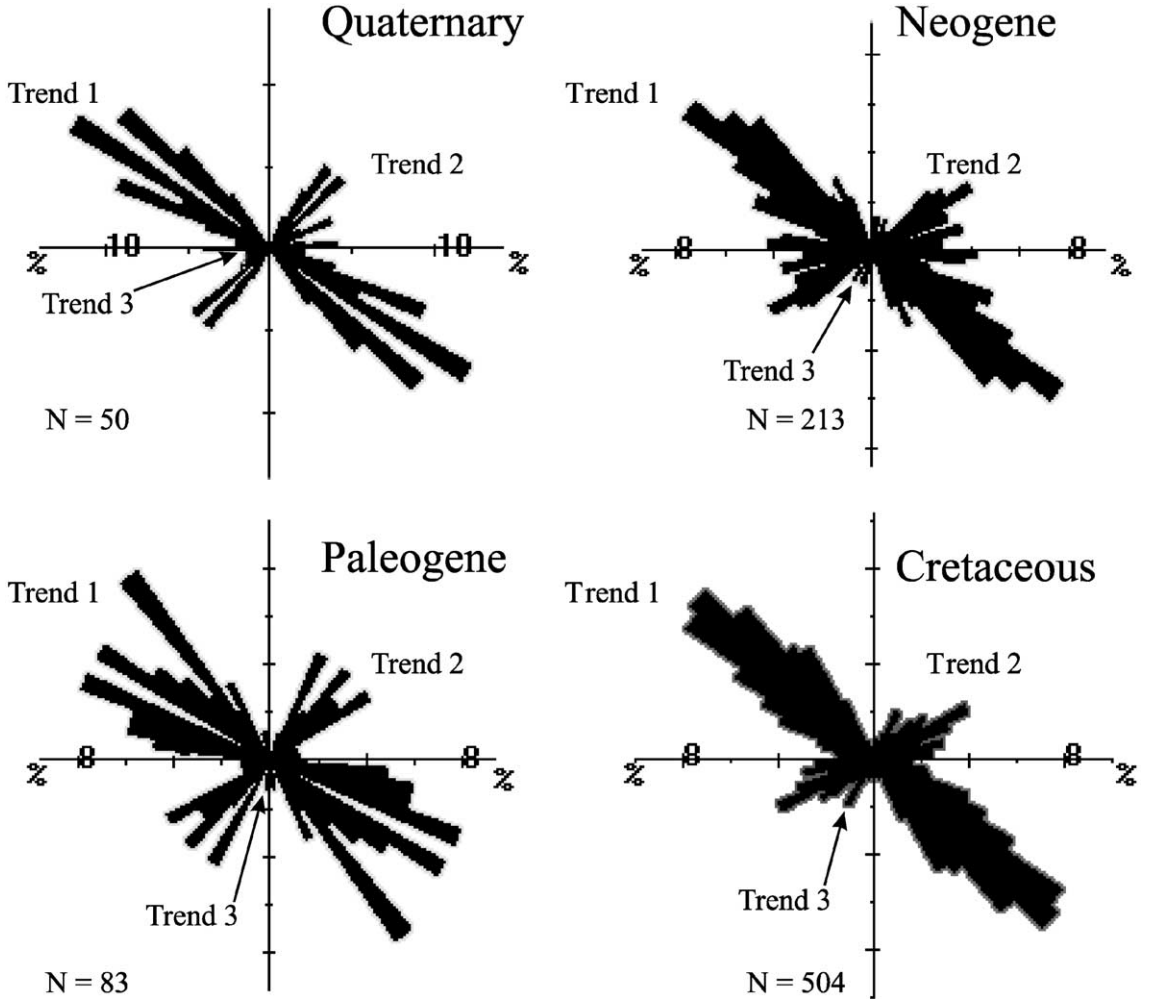

Fig. 6. Rose diagrams of the mapped lineaments that have been grouped based on the age of the bedrock cross-cut. Four, polygon feature class, geologic-unit age groups are cross-cut in this region. Each population of lineaments displays three trends as labeled in the figure.

Once the full mosaic of high-resolution radar images was mapped for lineament structures, the interpreted vector-feature lineament layer was exported into an Arc/Info arc-feature coverage and spatially analyzed with respect to existing bedrock geology coverages (Fig. 5). The bedrock geology served as a grouping constraint for the SAR-derived lineament dataset to evaluate the potential for changes in the stress regime with time. The bedrock geology coverages used are a small component (four adjacent tiles) of a larger multi-national, multi-year effort by the Main Research Information Computer Center (GlavNIVC), Russian Ministry of Natural Resources and the United States Geological Survey to digitally map all of Russia (area: 17,075,000 km^2)(AGI, 1998). The geologic geodataset coverages of the GlavNIVC/USGS effort were derived from the geologic maps of Nalivkin (1984). Other digital data resources and terrane maps (Nokleberg et al., 1997, 1998; Greniger et al., 1999) were reviewed as part of this study. The mapped lineament dataset was subdivided based on the age of the geologic unit polygon feature that the lineament cross-cut (Fig. 6). Statistical analysis with custom and modified C program computer code was performed on each division of the lineament dataset.

2.1. Numerical modeling

The numerical manifold method is a new numerical method that provides a unified framework for solving problems dealing with continuous media, discontinuous media, or a combination of both (Shi, 1995, 1997; Lin et al., 1999; Ku, 2001). There are three main features of the Numerical Manifold Method (NMM), block kinematics, a two-layer description of the modeling problem, and the simplex integration method. The two-layer description of the modeling problem consists of a physical mesh, which

Table 1

(A) General model parameters

Model	General parameters
1	Three-plate model: the Pacific plate is moving at a slower rate than predicted by Engebretson et al. (1985) to represent subduction while the Komandorskiy block is moving rapidly with collision occurring for 5.52 Ma.
2	Two-plate model: same conditions as model 1; a subducting Pacific plate and no Komandorskiy block.
3	Two-plate model: the rate of the Pacific plate is increased to that predicted by the Engebretson et al. (1985) model to represent more of an effect from collision in the NMM model.
4	Three-plate model: adds the Komandorskiy block to model 3. The Komandorskiy block is moving at a relatively slower rate, as indicated by the GPS measurements of Avé Lallement (personal communication, 2000).
5	Three-plate model: same as model 4 except the Komandorskiy starts off colliding with the Kamchatka Peninsula.

(B) Direction and rate parameters for numerical manifold method analysis

Model	Block 1	Block 2 (mm/year)	Block 3 (mm/year)	Orientation of blocks 2 and 3 (°)
Model 1	stationary	58.15	78.71	306.4[a]
Model 2	stationary	58.15	–	306.4[a]
Model 3	stationary	93.74[a]	–	306.4[a]
Model 4	stationary	93.74[a]	28.14[b]	306.4[a]
Model 5	stationary	93.74[a]	28.14[b]	306.4[a]

(C) Physical parameters for numerical manifold method analysis

Unit	Elastic modulus [E] [$E+10$ N/m^2]	Poisson's ratio [v] [average]	Compressive Strength [$E+08$ N/m^2]
Block 1 (granite)	1.7–7.6	−0.3–0.55 [0.04]	1.6–2.9
Block 2 (basalt)	4.9–11.2	−0.04–0.42 [0.17]	0.81–3.6
Block 3 (basalt)	4.9–11.2	−0.04–0.42 [0.17]	0.81–3.6

All values from (Johnson, 1970).

[a] From Engebretson et al. (1985).

[b] Modified from Avé Lallemant (personal communication, 2000).

is used to describe the physical boundaries including all discontinuities and a second mathematical mesh, which is a mesh of a regular geometric pattern. The number of mathematical elements was chosen according to computational accuracy requirements. The overlapping of these two descriptions is a manifold description (Lin et al., 1999). The Numerical Manifold Method (NMM) analysis was developed to model stress orientations in rock masses (Lin et al., 1999). Where rock masses often contain more than one fracture set, the geometric scale becomes more important as the different fracture sets may have different originating stress geometries. Lin et al. (1999) notes that it is essential to have reasonable estimates of the displacement field even with simplifications, since this field represents the fundamental basis for evaluating failure modes and resultant material stresses. To do this, they utilize the numerical manifold method to better constrain the displacement field. This method is effective when concerned with two fracture sets; a dominant and secondary set. The primary set is defined as the set with wider spacing that governs the overall kinematics of the rock mass. The secondary set is the source of some relative motion, but it is confined by the primary fracture set so the importance of the motion is irrelevant to the numerical calculation (Lin et al., 1999).

The numerical manifold method is a mixed continuum-discrete method. Fractures of the primary set are modeled as discontinuities, and those of the secondary set as a continuum. In this method, two model layers completely define the numerical problem; the first layer is the physical mesh layer, and the second is a mathematical mesh layer. Within the physical mesh layer are the problem boundaries and discontinuities affected by the primary fracture set. The mathematical mesh layer can be a mesh of a regular pattern geometry or combination of arbitrarily selected figures. The size and geometry of the mathematical mesh layer can be changed in accordance with the geometry of the modeling problem, accuracy desired in the solution, and physical properties of the

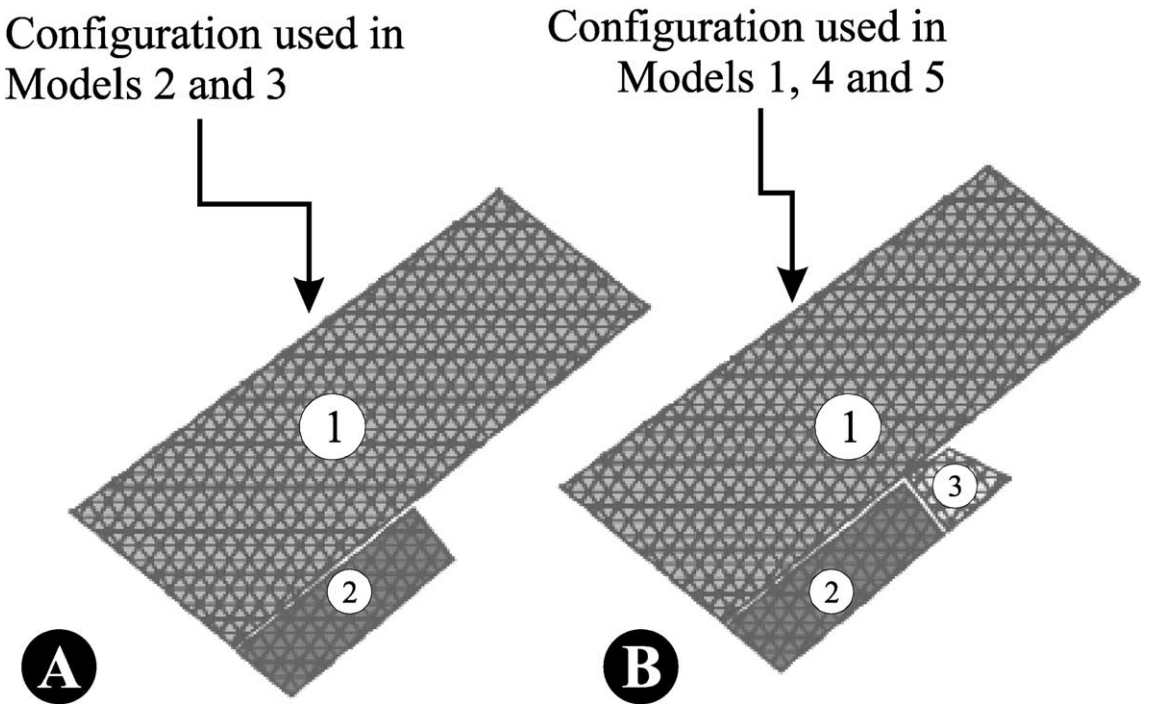

Fig. 7. Block configurations and numerical mesh for Numerical Manifold Method Analysis. Block 1 represents the Kamchatka Peninsula, block 2 is the Pacific plate and block 3 is the Komandorskiy Block. (A) Configuration used for models 2 and 3; (B) configuration used for models 1, 4 and 5.

region of interest (Lin et al., 1999). For this study, the size of the blocks is represented in real world dimensions for Kamchatka.

To complete an NMM analysis, a selected spatial region of rock mass is mathematically represented as an interconnected mesh of between 100 and 1000 triangular elements depending on the spatial and accuracy requirements of the solution. Within each triangular spatial element the displacement field is assumed to be linear and all physical parameters are constant. The physical parameters include elastic modulus (E), Poisson's ratio (v), and the compressive strength of the material (refer to Table 1 for the values used in our model). Initially the material behaves elastically until the principal stress exceeds the material yield strength and the material begins to fracture in accordance with the Mohr–Couloumb failure criteria (Lin et al., 1999). The NMM is primarily used for smaller scale numerical modeling applications, yet can be applied to the larger scale stress problem of plate tectonics. Changing the size and geometry of the mesh to match the spatial regions involved and selecting the appropriate physical parameters and stress orientations associated with tectonic applications does this. For our study, the size and geometry of the mesh reflect the actual size of the Kamchatka Peninsula and our tested geometry of plates and blocks in the region (Figs. 7 and 11).

3. Application of models

To investigate the two plate model of Engebretson et al. (1984, 1985) for describing the tectonic geometry of plates in the northwestern Pacific Basin, five representative points from the Cape Kamchatka Region were input used to calculate expected linear velocities and relative motion azimuths. Using a North America-fixed model, finite rotation poles were used to determine linear convergence vectors for the Pacific and Farallon oceanic plates for the past 43 Ma. Assuming that the North American plate is fixed simplifies the numerical model and allows the com-

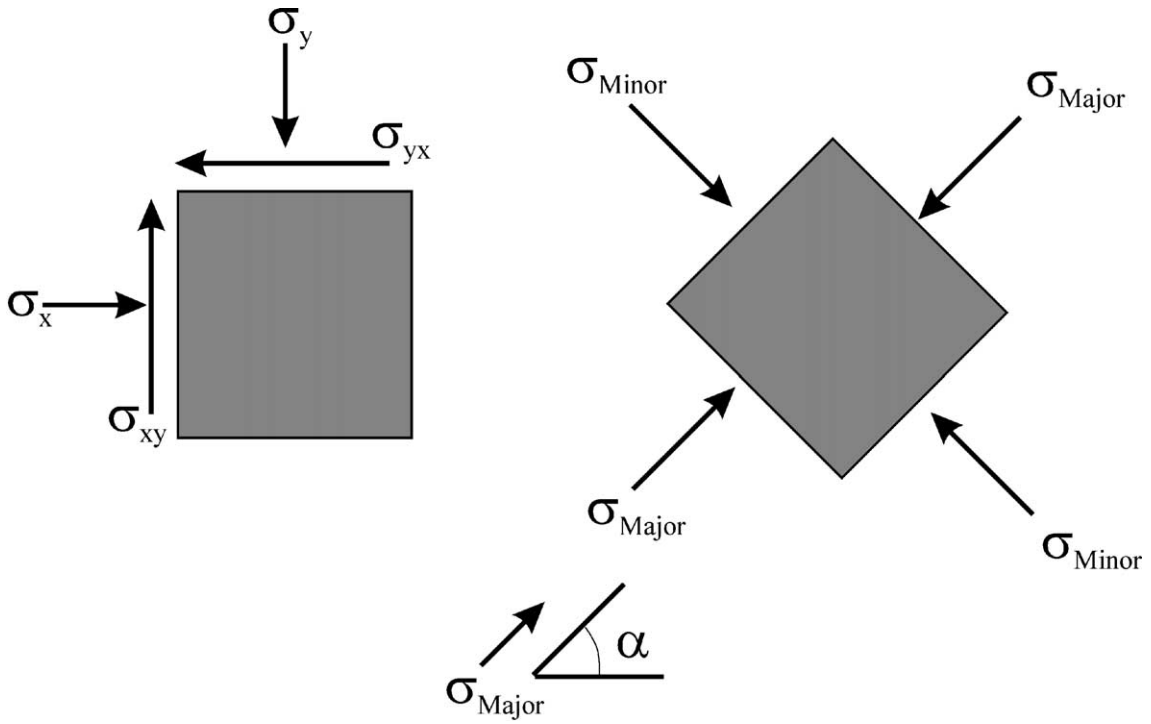

Fig. 8. Representation of the stresses as described for determining the NMM model. Refer to Eqs. (1) and (2) (from Ku, 2001).

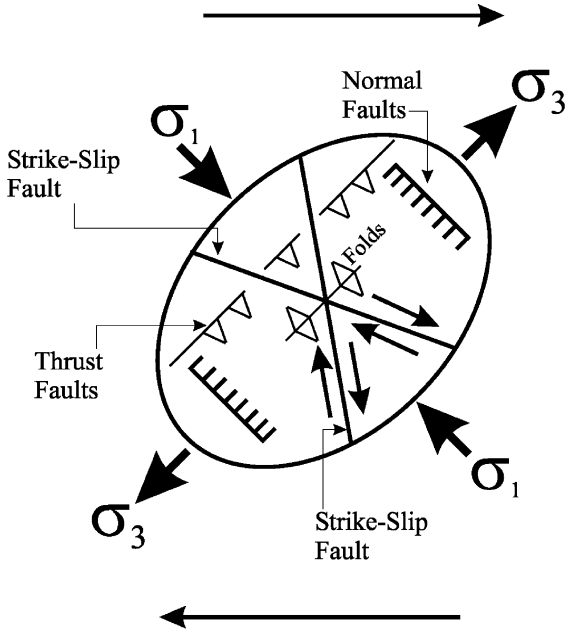

Fig. 9. Diagram representing the structural pattern produced by dextral simple-shear (after Park, 1988).

parison of numerical results with features formed by the interaction of the Kamchatka Peninsula and interacting oceanic plates. It is assumed that these convergence vectors represent a proxy for relative stresses in this region.

To forward model the two-plate geometry (Chapman and Solomon, 1976; Engebretson et al., 1984, 1985) and three-block geometry configuration (Mackey et al., 1997; Avé Lallemant et al., 1999; Oldow et al., 1999), Numerical Manifold Method analysis was employed. For the geometric configuration of blocks in our models, we starting with approximations to previously described plate configurations in the region as noted above. Two-block configurations and three-block configurations (Fig. 7) were tested in five NMM models where velocity varied in the moving blocks (Table 1). In all models block 1, representing the Kamchatka Peninsula, (North American plate) is held stationary. Block 2 represents the Pacific plate moving in the northwest direction, specifically with orientation of 306.4°. The velocity of block 2 changes in the different models to represent the stress influence from a predominantly subducting or colliding plate. Block 3 represents the proposed Komandorskiy Block, also moving in the northwest direction (orientation 306.4°) with velocity changing to represent constant collision or the onset of collision for the duration of the model. All models are run for 100 time steps corresponding to a total time duration of 5.58 Ma.

The mesh used for the NMM analysis contained 982 triangular elements for the three-block models and 936 triangular elements for the two-block models (Fig. 7). For each element in the mesh σ_x, σ_y, and σ_{xy} stresses were calculated, where σ_x is the normal stress in the x direction, σ_y is the normal stress in the y direction, and σ_{xy} is the stress orientation in the xy plane (Fig. 8). Once σ_x, σ_y, and σ_{xy} were calculated at the center of each triangular element, these forces were used to define the maximum (σ_1) and minimum (σ_3) principal stress vectors using Eqs. (1) and (2). The stress vectors

$$\sigma_1 = \frac{1}{2}(\sigma_x + \sigma_y) + \sqrt{\left(\sigma_{xy}^2 + \frac{1}{4}(\sigma_x - \sigma_y)^2\right)} \quad (1)$$

$$\sigma_3 = \frac{1}{2}(\sigma_x + \sigma_y) - \sqrt{\left(\sigma_{xy}^2 + \frac{1}{4}(\sigma_x - \sigma_y)^2\right)} \quad (2)$$

were used to predict orientations of different faults types for each model in accordance with the Andersonian theory of faulting (Fig. 9), which were then compared to the orientations of the observed lineaments (Sylvester, 1988).

To compare the results of NMM modeling with the observations of lineaments at Cape Kamchatka, the orientation values for the principle stress at each triangular element were used to calculate the predicted mean orientations for a pair of conjugate strike–slip

Table 2
Observed and predicted mean orientations for faults based on NMM modeling

Model	Predicted thrust fault orientation (°)	Predicted conjugate strike slip orientation	
		Set 1 (°)	Set 2 (°)
Model 1	211 ± 1.8	241 ± 1.8	301 ± 1.8
Model 2	203 ± 2.1	233 ± 2.1	293 ± 2.1
Model 3	248 ± 1.2	278 ± 1.2	338 ± 1.2
Model 4	248 ± 1.2	278 ± 1.2	338 ± 1.2
Model 5	241 ± 1.4	271 ± 1.4	310 ± 1.4
Observed	210 ± 1.4	240 ± 1.4	310 ± 1.4

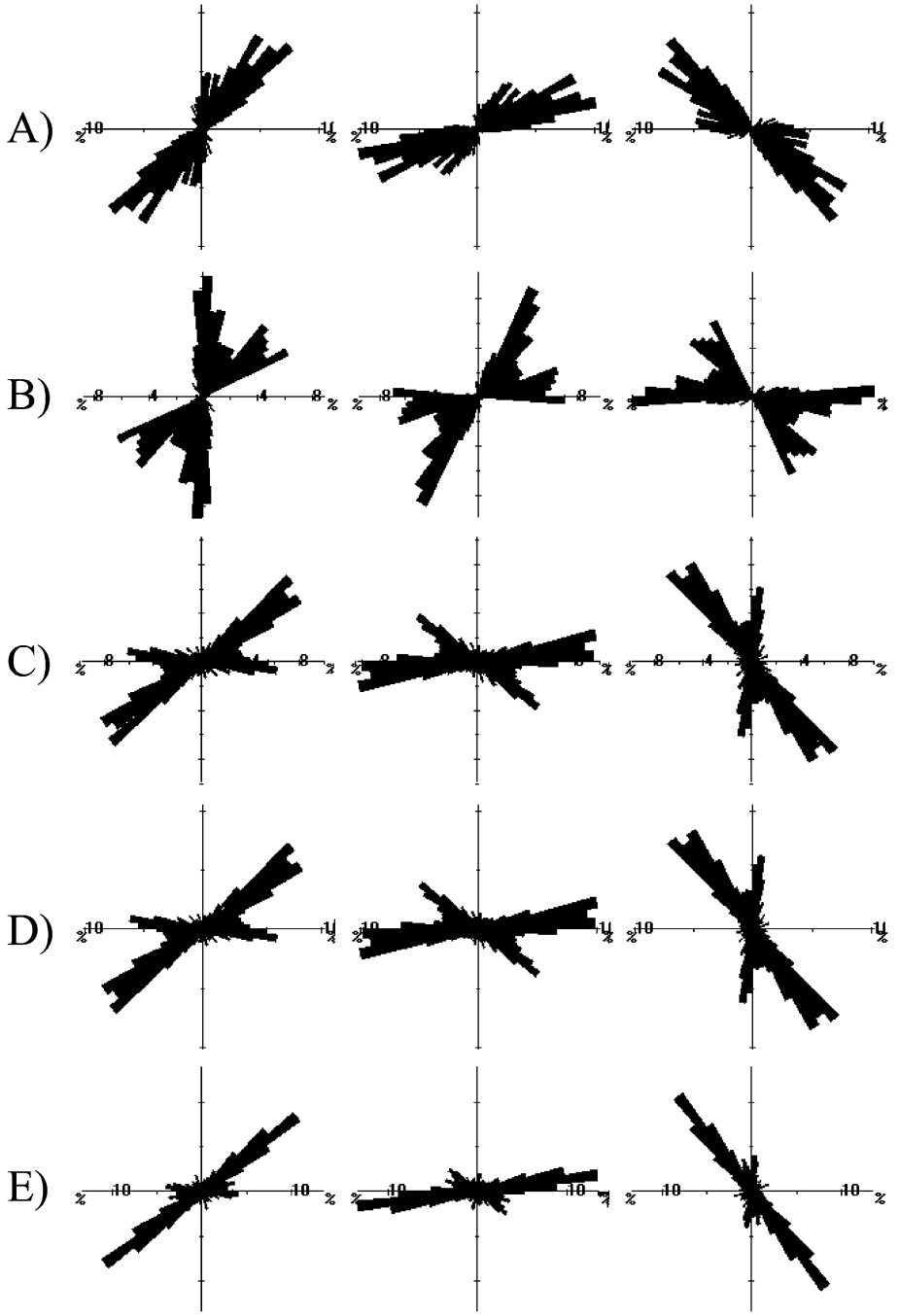

Fig. 10. Rose diagrams depicting the predicted orientations of thrust, strike–slip and conjugate strike–slip faults based on NMM analysis; BIN size = 5°. Each row shows the results of one model; column 1 is thrust faults and columns 2 and 3 showing are strike–slip faults. (A) Model 1, $N = 798$; (B) model 2, $N = 793$; (C) model 3, $N = 797$; (D) model 4, $N = 800$; (E) Model 5, $N = 802$.

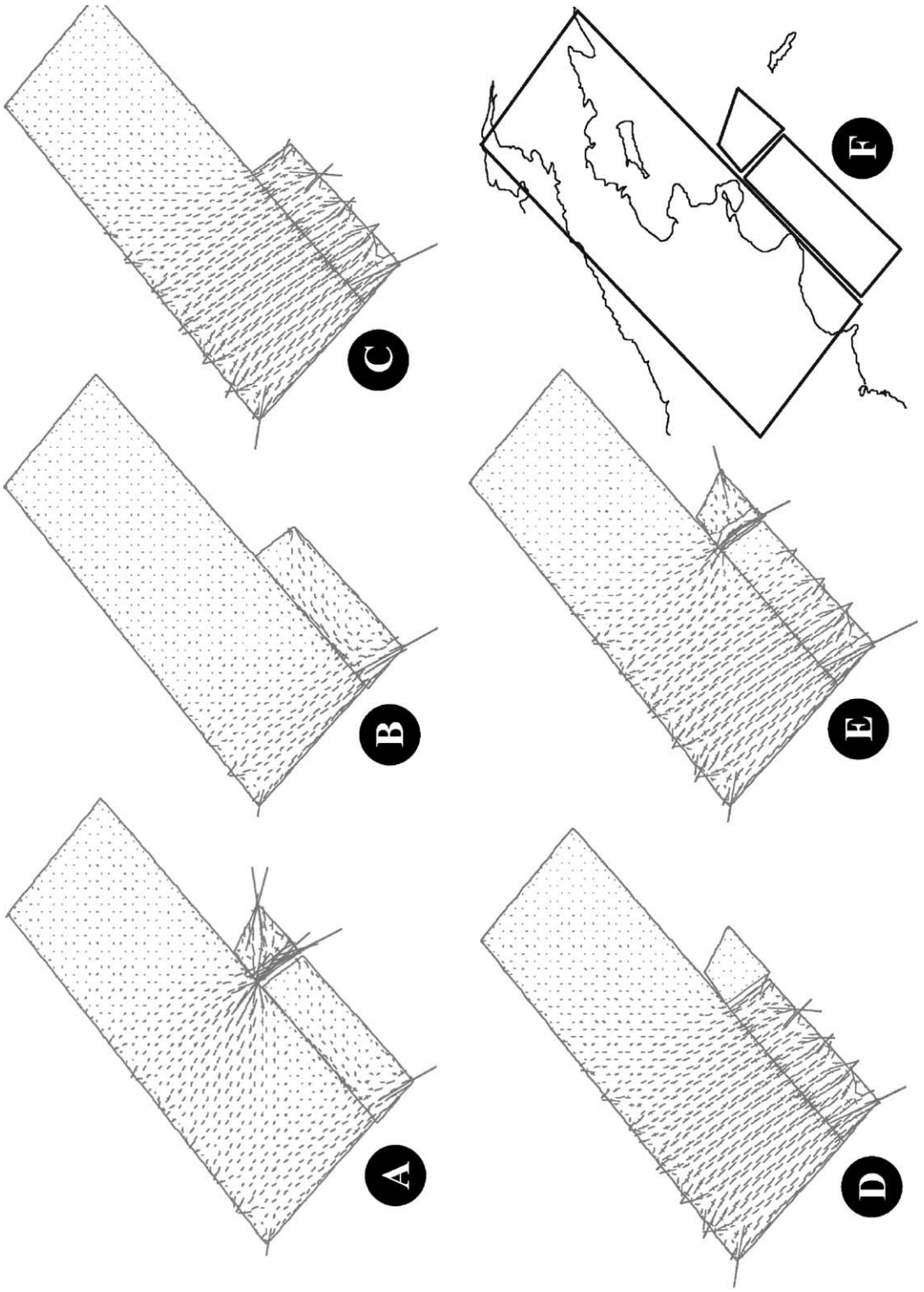

Fig. 11. Orientation principal major and minor stresses at 5.58 Ma as determined by Numerical Manifold Method analysis for all models. Lengths of σ_1 and σ_3 are scaled by respective magnitudes and are centered within their respective triangular mesh element. (A) Model 1, (B) model 2, (C) model 3, (D) model 4, (E) model 5, (F) model blocks with Kamchatka coastline for reference.

faults and thrust faults following the Andersonian model of faulting (Table 2, Fig. 10). The mean orientations for each fault type were calculated using GeOrient and represents the spherical mean that is a best-fit estimate for non-polar azimuthal data. In addition to the mean orientations of the features formed in response to the stress, the spatial location of the stress vectors needs to be considered in evaluating each of the models (Fig. 11). Fig. 11 shows the orientation for principal major and minor stresses (length scaled by magnitude) in each triangular element at the end-stage of the NMM analysis for each model. The spatial distribution of the larger stress vectors varies throughout block 1 (Kamchatka Peninsula) amongst the five models. For example, model 1 and model 5 are the only models which show large stress vectors at Cape Kamchatka; whereas model 2 only shows large stress vectors just north of Shipunskiy Peninsula (southern region of model space). Since the predicted fault orientations are based on σ_1 and σ_3 in each triangular element and then grouped to determine mean orientations, the spatial location of each element needs to be considered when evaluating the model results with the observed data. The similarity between model 1 and observed data from SAR indicates that the model 1 parameters acceptably describe the tectonic configuration in the northwestern Pacific basin. That is, three tectonic blocks interacting, where the Pacific plate is subducting and the Komandorskiy block is colliding with the Kamchatka Peninsula.

4. Results

The lineaments were grouped based on the age of the rock units they crosscut using topologically based spatial overlay operations to create the new geo-data sets. Spatial locations of lineaments were quantitatively compared with orientations of the observed structural features. The mean orientations of these lineaments are shown in the last row of Table 2. Using a UTM map projection (UTM Zone 57), lineament data elements were calculated using planar geometry-based numerical calculations. This Cartesian northings–eastings meter surface preserves geoid surface angles exactly and introduces only minor distortions to distances. Lineament orientation, length, parallel and perpendicular pacing-centroid, and spatial offset data for each lineament were calculated using a technique modified from Clark and Wilson (1994).

Comparing the predicted orientations from the two-plate model with the orientations of the mapped lineaments, there is reasonable agreement with faults cross-cutting Quaternary, Paleogene, and possibly Neogene age rocks. Since the time frame defined by the finite rotation poles of Engebretson et al. (1984) does not correspond directly with geologic time periods, a direct comparison is difficult. Our observed data is somewhat consistent with the Engebretson et al. (1984) model in the Quaternary and Late Paleogene; however, there is little correlation with data for the Neogene and Early Paleogene. The similarities with primary trends in predicted (from Engebretson et al., 1984 model) and observed lineament orientation may suggest that the Engebretson et al. (1984) model accurately predicts regional stress at Cape Kamchatka, thus indicating that the dominant stress in the region may be from the interaction between the Pacific and North American plates. In this interpretation, the disagreement with the trends through most of the Neogene is due to the formation and movement of the Komandorskiy–Aleutian Arc block. In addition, within the framework of this interpretation, the observed lineament azimuth distribution accurately and quantitatively records, and may be interpreted as, a proxy for regional lithospheric stress.

Because Kamchatka is comprised of accreted terranes, the age of the rock may not be as important as its geographic location with respect to the plate boundary. Cretaceous rock units compose the most outboard unit in the southern section of the study area. Therefore the signature of modern stresses occurs in the oldest rocks in the study region. This may be one reason why the majority of the lineaments are found in the Cretaceous-age rocks. Another may be that the spatial geographic extent of the Cretaceous units within the SAR-based region of investigation is the largest followed by the Neogene. The Quaternary-age units are wide ranging, but also represent recent volcanism possibly erasing structures. In addition, many of the Quaternary units are in the region of volcanic centers, which was avoided during mapping due to layover effects in the radar data.

Although there is some agreement with our mapped data and the model data of Engebretson et al.

(1984, 1985) as noted above, there is not total agreement across time or with secondary and tertiary orientation trends. These inconsistencies, lead us to explore more complex plate configurations invoking the collisions of the Komandorskiy block using NMM analysis. As discussed above five tectonic models were explored with the results compared to our mapped results. The predicted orientations for model 1 match trends in the observed data fairly well. The primary and secondary trends of observed lineaments correlate reasonably well with the orientations for the conjugate pairs of strike–slip faults when comparing rose diagram distributions and mean orientations. The third trend of observed lineaments correlates very well with thrust faults when comparing mean orientations. The location of stress vectors closely matches the location of the mapped lineaments on the Kamchatka Peninsula (Block 1).

The other NMM model results for two-block and three-block configurations did not correlate as well as model 1 with the observed data set. The two-plate models (models 2 and 3) do not accurately predicting the geographic location of the larger stress vectors that correspond to the location of mapped lineaments. The remaining three-plate models also do not agree as well as model 1. In model 4 where the Komandorskiy block initiates collision in the final time step, the end result is no different than model 3, a two-plate model. Model 5, uses the same parameters as model 4, however the Komandorskiy block starts colliding at the beginning of the model run, which results in a narrower predicted mean orientation for the different fault types. Agreement was found between the predicted orientation for conjugate strike slip faults with mapped observations, however the overall trends for the other fault types does not agree.

When the lineament data set is spatially divided into groups based on the age of the youngest rock unit cross-cut, a similar pattern of three trends is seen correlating to the different fault types. However, there is some variation of the mean orientation for each fault type indicating that tectonic rotation may have occurred in the region as well as the possibility of some over printing from more recent deformation events. The more inboard units still match the overall picture predicted by model 1. Observed variation from this predicted orientation may be explained by pre-existing faults formed from a past stress regime of collision like that suggested by Tapponnier et al. (1982) and were subsequently rotated by one or more of the methods for tectonic rotation as described by MacDonald (1980). In the inboard units overprinting of the modern stress field may have occurred as indicated by agreement between NMM model 1 predictions and observed trends.

5. Conclusion

In this study, one objective was to create and validate a method of regional mapping of linear structural features from high-resolution radar data. The fusion of geo-data sets within a geographical information system quantifies the relationship between structural features and geology in the tectonically active region of the northwestern Pacific Basin. This information provides a test for models of plate motion and plate configuration in the region—a topic of debate for the past three decades. The Geographical Information Systems method of quantifying the linear features is applicable and useful as a grouping process, but does not provide absolute dating of the lineaments. Subdividing the lineaments into groups based on the age of the bedrock they cross-cut is useful for determining geographic extent and clustering of lineaments in addition to looking for lineament trends within a given age unit. Our study suggests that the most likely tectonic configuration in the northwestern Pacific basin is one that incorporates the existence of the Komandorskiy block. Our modeled results for a three-plate configuration with the Pacific plate subducting and the Komandorskiy block (model 1) moving rapidly and colliding with the Kamchatka Peninsula best matched the mapped lineament data. In comparison with proposed two-plate models and our own two-plate models, our observational data correlate well in some areas, but poorly in others, whereas our three-plate model had very good agreement in all areas. Movement of the Komandorskiy block has resulted in a detectable proxy represented by SAR-observable lineament structures in the Cape Kamchatka region of the Kamchatka Peninsula. In the future, we plan to add the depth dimension to our NMM model and numerically model basal shear. We also plan to examine other remotely sensed data of the area to continue mapping structural features to add to

our database. The addition of these data will aid in the evaluation of future models.

Acknowledgements

We wish to thank the Editor and the reviewers of this manuscript, Dr. Eric Geist and Professor J.S. Oldow, their work and suggestions significantly improved the quality of our manuscript. Funding for this work came from National Science Foundation award EAR97-06446 and the University of Pittsburgh. S.B.Z. McElfresh would like to thank the Pennsylvania Space Grant Consortium for funding some of this work. All SAR images come from the Alaska SAR Facility. The help and support of the Alaska SAR Facility, NASA, NSF and the Arctic Research Consortium of the United States (ARCUS) are gratefully acknowledged. We wish to thank Dr. N. Tsukanov for his detailed discussions of this region during his visit to the University of Pittsburgh, with support from EAR97-06446, and the generous cooperation of Dr. Tsukanov in allowing us access to his analysis of the geology and tectonics of the Cape Kamchatka region.

References

AGI, 1998. Natural Resources of Russia, Main Research Information Center (GlavNIVC), Russian Ministry of Natural Resources, CDROM.

Avé Lallemant, H.G., Oldow, J.S., 2000. Active displacement partitioning and arc-parallel extension of the Aleutian volcanic arc based on Global Positioning System geodesy and kinematic analysis. Geology 28 (8), 739–742.

Avé Lallemant, H.G., Oldow, J.S., Ferranti, L., Mashio, L., Comstock, J.E., Lewis, D.S., 1999. Displacement partitioning, trench parallel stretching and westward migration of the Aleutian Arc and collision with Kamchatka: Part 1. Structural analysis, (abstract). Eos Trans. AGU 80, F947.

Chapman, M.E., Solomon, S.C., 1976. North American–Eurasian plate boundary in Northeast Asia. J. Geophys. Res. 81, 921–930.

Clark, C.D., Wilson, C., 1994. Spatial analysis of lineaments. Comput. Geosci. 20, 1237–1258.

Cook, D.B., Fujita, K., McMullen, C.A., 1986. Present-day plate interactions in northeast Asia: North American, Eurasian, and Okhotsk plates. J. Geodyn. 6, 33–51.

Didenko, A., Harbert, W., Stavsky, A., 1993. Paleomagnetism of Khatyrka and Mayintsky supperterranes, Koryak highlands, far eastern Russia. Tectonophysics 220, 141–155.

Engebretson, D.C., Cox, A., Gordon, R.G., 1984. Relative motion between oceanic plates of the Pacific Basin. J. Geophys. Res. 89, 10291–10310.

Engebretson, D.C., Cox, A., Gordon, R.G., 1985. Relative motions between oceanic and continental plates in the Pacific Basin: Special Paper 206.

Gaeidicke, C., Alexeiev, D., Tsukanov, N., Baranov, B., Freitag, R., 1998. Evolution of the Kumroch Range and the Kamchatsky Mys Peninsula (Eastern Kamchatka) in the Late Cretaceous to Cenozoic. 6th Zoneshain Conference on Plate Tectonics and Europrobe Workshop on Uralides: Moscow, Russia, 207.

Gaeidicke, C., Alexeiev, D., Baranov, B., Seliverstov, N., Alexeiev, D., Tsukanov, N., Freitag, R., 2000. Structure of an active arc–continent collision area: the Aleutian–Kamchatka junction. Tectonophysics 325, 63–75.

Geist, E.L., Scholl, D.W., 1994. Large-scale deformation related to the collision of the Aleutian Arc with Kamchatka. Tectonics 13, 538–560.

Greniger, M.L., Klemperer, S.L., Nokleberg, W.J., 1999. Geographic Information Systems (GIS) Compilation of Geophysical, Geologic, and Tectonic Data for the Circum-north Pacific, US Geological Survey Open-File Report 99-422.

Grigoriev, N., Krylov, K.A., 1992. Accreted Mesozoic Oceanic Terranes of Koryak Supperterrane, Northeastern Russia. In: Thurston, D.K., Fujita, K. (Eds.), Proceedings International Conference on Arctic Margins. US Department of the Interior, Anchorage, AK, pp. 17–222.

Heiphetz, A., Harbert, W., Savostin, L., 1992a. Reconnaissance Paleomagnetism of the Olyutorsky Supperterrane, NE Russia. In: Thurston, D.K., Fujita, K. (Eds.), Proceedings International Conference on Arctic Margins. US Department of the Interior, Anchorage, AK, pp. 223–228.

Heiphetz, A., Harbert, W., Layer, P., 1992b. Preliminary Reconnaissance Paleomagetism of some Late Mesozoic Ophiolites, Kuyul Region, Northern Koryak Supperterrane, Russia. In: Thurston, D.K., Fujita, K. (Eds.), Proceedings International Conference on Arctic Margins. US Department of the Interior, Anchorage, AK, pp. 229–234.

Johnson, A.M., 1970. Physical Processes in Geology. Freeman, San Francisco, CA, 202 pp.

Ku, C.-Y., 2001. Modeling of jointed rock masses based on the numerical manifold method, PhD Thesis, School of Engineering, University of Pittsburgh, 221 pp.

Levashova, N.M., Shapiro, M.N., Bazhenov, M.L., 1998. Late Cretaceous paleomagnetic data from the Median Range of Kamchatka, Russia: tectonic implications. Earth Planet. Sci. Lett. 163, 235–246.

Lin, J.-S., Koo, C.-Y., Chern, J.-C., 1999. Manifold method of rock masses containing joints of two sets. Proceedings of ICADD-3, Third International Conference on Analysis of Discontinuous Deformation—from Theory to Practice. Vail, Colorado, pp. 231–242.

MacDonald, W.D., 1980. Net tectonic rotation, apparent tectonic rotation, and the structural tilt correction in paleomagnetic studies. J. Geophys. Res. 85, 3659–3669.

Mackey, K.G., Fujita, K., Gunbina, L.V., Kovalev, V.N., Imaev, V.S., Koz'min, B.M., Imaeva, L.P., 1997. Seismicity of the

Bering Strait region: evidence for a Bering Block. Geology 25, 979–982.

Nalivkin, D.V., 1984. Geologic Map of Russia. USSR Research Geological Institute (VSEGEI), Leningrad.

Nokleberg, W.J., Bundtzen, T.K., Dawson, K.M., Eremin, R.A., Goryachev, N.A., Koch, R.D., Ratkin, V.V., Rozenblum, I.S., Shipikerman, V.I., Frolov, Y.F., Gorodinsky, M.E., Melnikov, V.I., Diggles, M.F., Ognyanov, N.V., Petrachenko, E.D., Petrachenko, R.I., Pozdeev, A.I., Ross, K.V., Wood, D.H., Grybeck, D., Khanchuk, A.I., Kovbas, L.I., Nekrasov, I.Y., Sidorov, A.A., 1997. Significant Metalliferous and Selected Non-Metalliferous lode Deposits and Placer Districts for the Russian Far East, Alaska, and the Canadian Cordillera. US Geological Survey Open File Report 96-513-B.

Nokleberg, W.J., West, T.D., Dawson, K.M., Shipikerman, V.I., Bundtzen, T.K., Parfenov, L.M., Monger, J.W.H., Ratkin, V.V., Baranov, B.V., Byalobzhesky, S.G., Diggles, M.F., Eremin, R.A., Fujita, K., Gordey, S.P., Gorodinsky, M.E., Goryachev, N.A., Feeney, T.D., Frolov, Y.F., Grantz, A., Khanchuk, A.I., Koch, R.D., Natalin, B.A., Natapov, L.M., Norton, I.O., Patton, Jr., W.W., Plafker, G., Pozdeev, A.I., Rozenblum, I.S., Scholl, D.W., Sokolv, S.D., Sosunov, G.M., Stone, D.B., Tabor, R.W., Tsukanov, N.V., Vallier, T.L., 1998. Summary terrane, mineral deposit, and metallogenic belt maps of the Russian Far East, Alaska, and the Canadian Cordillera. US Geological Survey Open File Report 98-136.

Oldow, J.S., Lewis, D.S., Avé Lallemant, H.G., Ferranti, L., Mashio, L., Comstock, J.E., Freymueller, J., 1999. Displacement partitioning, trench parallel stretching and Westward Migration of the Aleutian Arc and Collision with Kamchatka: Part 2. GPS Geodetic analysis. Eos Trans., AGU 80, F947.

Olmsted, C., 1994. Scientific SAR User's Guide, Volume ASF-SD-003, Alaska SAR Facility.

Park, R.G., 1988. Geological Structures and Moving Plates. Chapman & Hall, New York, 337 pp.

Perchesky, D.M., Levashova, N.M., Shapiro, M.N., Bazhenov, M.L., Sharonova, Z., 1997. Paleomagnetism of the Paleogene volcanic series of the Kamchatksy Mys, East Kamchatka: the motion of an active island arc. Tectonophysics 273, 219–237.

Riegel, S.A., Fujita, K., Koz'min, B.M., Imaev, S., Cook, D.B., 1993. Extrusion tectonics of the Okhotsk plate, northeast Asia. Geophys. Res. Lett. 20, 607–610.

Shi, G.-H., 1995. Numerical manifold method. Proceeding of the Working Forum of the Manifold of Material Analysis, pp. 1–128.

Shi, G.-H., 1997. Numerical manifold method. Proceeding of the Second International Conference on the Analysis of Discontinuous Deformation, Kyoto, Japan, pp. 1–36.

Sylvester, A.G., 1988. Strike–Slip Faults. Geol. Soc. Am. Bull. 100, 1666–1703.

Tapponnier, P., Peltzer, G., Le Dain, A.Y., Armijo, R., Cobbold, P., 1982. Propagating extrusion tectonics in Asia: new insights from simple experiments with plasticine. Geology 10, 611–616.

Watson, B.F., Fujita, K., 1985. Tectonic evolution of Kamchatka and the Sea of Okhotsk and implications for the Pacific Basin. In: Howell, D.G. (Ed.), Tectonostratigraphic Terranes of the Circum-Pacific Region, vol. 1. The Circum-Pacific Council for Energy and Mineral Resources, Houston, pp. 333–348.

Zimmerman, S.B., 2000. GIS Analysis and Stress Modeling of Tectonic Blocks At Cape Kamchatka, Russia using Principal Stress Proxies from High-Resolution SAR: New Evidence for the Komandorskiy Block, MS thesis, University of Pittsburgh, 357 pp.